egory had a larger mass of muscle in their pulmonary arteries, heavier cardiac right ventricles, and more retained brown fat and hepatic erythropoiesis than did SIDS victims with a smaller volume of glomic tissue (Table 2). The glomic tissue volume of 63 percent of the SIDS victims was classified as subnormal because their ratios of glomic volume to body weight were in the lower 10th percentile of values for the control infants, that is, less than 0.64. SIDS victims in this category had no significant correlations between the ratios of glomic volume to body weight and the various parameters of chronic hypoventilation and hypoxemia. Mean values for the ratio of volume nerve fibers to volume carotid body glomic tissue were similar in age-matched SIDS victims and controls.

Our study indicated that 63 percent of victims of SIDS has a subnormal volume and 23 percent an enlarged volume of glomic tissue in their carotid bodies. These abnormalities were not due to a failure of nerve fibers to grow into the organ. Evidences of antecedent chronic alveolar hypoxia and hypoxemia were found in both groups but were more severe in the victims with the enlarged glomic tissue. Neither of the carotid body abnormalities in the SIDS victims are easy to interpret because it is not known which structures in the organ comprise the various functional components of the chemoreceptor apparatus (*12, 13*). Glomic tissue is often hyperplastic in animals and human beings who are chronically hypoxemic, but it is not known whether this change is a primary or a secondary response to the blood gas abnormality (*8, 12*). The defect that is responsible for the subnormal volume of glomus cells in many SIDS victims might be primary in the organ or it could reside in brain stem respiratory centers and their efferent or afferent connections to the carotid body. Findings in our study give little basis for choice. However, the finding of both hyperplastic and hypoplastic glomic tissue in various SIDS victims increases the possibility that diverse mechanisms are involved in their deaths, even if apneic episodes remain a common final pathway.

A subnormal volume of carotid glomic tissue was less common in infected than in noninfected victims. In addition, there are other differences between the two groups. Infected victims are older at death, have smaller thymus glands, and have somewhat milder features of chronic hypoventilation and hypoxemia than do noninfected victims (*5*). This might suggest that a smaller proportion of deaths in infected victims are due to the hypoventilation-apnea mechanism. However, infections increase both the frequency and the duration of apneic episodes during sleep in susceptible infants, so abnormalities in respiratory control remain a likely explanation for many deaths in both infected and noninfected victims (*2, 14*).

RICHARD L. NAEYE
M. S. Hershey Medical Center, Pennsylvania State University, Hershey 17033
RUSSELL FISHER, MONIQUE RYSER
PHILIP WHALEN
Office of the Chief Medical Examiner, State of Maryland, Baltimore 21201

References and Notes

1. A. Steinschneider, *Pediatrics* **50**, 646 (1972).
2. A. Stevens, *Am. J. Dis. Child.* **110**, 243 (1965).
3. A. Guilleminault, R. Eldridge, W. Dement, *Science* **181**, 856 (1973); E. Lugaresi, C. Coccagni, M. Mantovani, *et al.*, *Bull. Physio-Pathol. Respir.* **8**, 1103 (1972).
4. R. Naeye, *N. Engl. J. Med.* **289**, 1167 (1973).
5. ———, P. Whalen, M. Ryser, R. Fisher, *Am. J. Pathol.*, in press.
6. R. Naeye, *Science* **186**, 837 (1974).
7. ———, in preparation.
8. D. Heath and C. Edwards, *Geriatrics* **26**, 110 (Dec. 1971).
9. H. Chalkley, *J. Natl. Cancer Inst.* **4**, 47 (1943).
10. M. Dunnill, in *Recent Advances in Clinical Pathology*, S. C. Dyke, Ed. (Churchill, London, 1968), p. 401.
11. A. Sevier and B. Munger, *J. Neuropathol. Exp. Neurol.* **24**, 130 (1965).
12. T. Briscoe, *Physiol. Rev.* **51**, 437 (1971).
13. D. McDonald and R. Mitchell, *J. Neurocytol.* **4**, 177 (1975).
14. A. Steinschneider, in *SIDS 1974, Proceedings Francis E. Camps International Symposium on Sudden and Unexpected Deaths in Infancy*, R. R. Robinson, Ed. (Canadian Foundation for the Study of Infant Death, Toronto, 1974), p. 117.
15. Supported by PHS grant HL 14297 and contract NO1-HD-4-2817.

22 September 1975; revised 31 October 1975

Proviral DNA of Moloney Leukemia Virus: Purification and Visualization

Abstract. *Closed-circular proviral DNA of Moloney leukemia virus has been purified from a 10^7 excess of cellular and mitochondrial DNA. The DNA can be visualized in the electron microscope and has the contour length of a molecule with a molecular weight of about 5.5×10^6. Electron microscopic observation of a hybrid between viral RNA and this circular DNA confirms the viral origin of this molecule.*

The viral DNA of RNA tumor viruses is found in several forms shortly after infection of a susceptible cell. Of great interest is a closed-circular, double-stranded superhelical form of the viral DNA shown to exist in cells infected by Rous sarcoma virus (*1*) or Moloney leukemia virus [M-MuLV (*2*)]. Its characterization has been impeded by the low amounts of this DNA that can be isolated from infected cells.

Nine hours after infection by M-MuLV, one closed-circular molecule of virus can be isolated per ten cells in a culture in which all the cells have been productively infected. This proviral DNA is therefore present with a 10^7-fold excess of nuclear and mitochondrial DNA (mtDNA). Several procedures have been used for the enrichment and purification of the viral DNA (*1, 2*). The Hirt extraction procedure (*3*) followed by centrifugation in a mixture of ethidium bromide and cesium chloride (EtBr-CsCl) (*4*) afforded a 700-fold enrichment. These steps leave the closed-circular viral DNA still contaminated by more than a 10,000-fold excess of mtDNA, whose similar closed-circular structure results in its copurification in the isopycnic centrifugation.

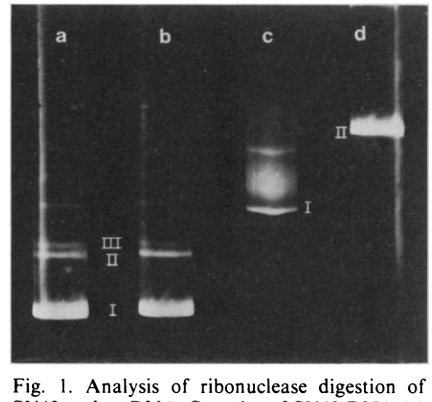

Fig. 1. Analysis of ribonuclease digestion of SV40 and mtDNA. Samples of SV40 DNA (a) and mtDNA (c) were subjected to electrophoresis directly in agarose gels (*15*). Equivalent samples were digested with ribonuclease A (50 μg/ml, 1 m*M* tris, 0.5 m*M* EDTA, *p*H 7.4, 1 hour at 37°C) before electrophoresis on parallel gels (b and d). (I) closed-circular DNA; (II) nicked-circular DNA; (III) linear DNA.

We have developed two methods for the further enrichment of the viral DNA: one generally applicable to all such closed-circular DNA's and the other particularly useful for the M-MuLV genome studied here. The first procedure depends on the existence of ribonucleotide linkages that exist in mtDNA (*5*). Analysis in an alkaline sucrose gradient has shown that these are absent from most if not all closed-circular proviral DNA molecules (*1, 2*). We also rely on the sensitivity of duplexed RNA to ribonuclease when digestion is performed at low ionic strength (*6*). Digestion of mtDNA with ribonuclease in low ionic strength should nick the closed-circular form of this DNA at any ribonucleotide linkage, and leave intact other closed-circular molecules lacking this linkage.

SV40 DNA, a closed-circular molecule which lacks ribonucleotide linkages, is resistant to ribonuclease and continues to migrate as closed-circular DNA after enzyme treatment (Fig. 1). In contrast, 98 to 99 percent of mtDNA now migrates like nicked-circular mtDNA in an agarose gel. This nicked mtDNA can be removed from the remaining closed-circular DNA by a subsequent cycle of CsCl-EtBr centrifugation. Control hybridization experiments confirmed that virtually all the proviral DNA was unaffected by ribonuclease treatment and continued to band as closed-circular DNA.

The ribonuclease treatment leaves a 50- to 100-fold excess of mtDNA, making possible the visualization of proviral DNA. Figure 2 shows the size distribution of such preparations as visualized in the electron microscope. The size distribution of all circular molecules smaller than mtDNA, which itself served as an internal size marker on all grids, is shown in Fig. 2, a and b (*7*). Certain preparations from mock-infected cells yield a distribution of molecules from 0.1 to 0.4 the length of mtDNA (Fig. 2a), while other preparations of mock-infected cells failed to yield molecules of less than the length of mtDNA. The origin of these molecules is unclear. They are larger than the previously observed small circular DNA's of HeLa cells, which are less than 0.1 the length of mtDNA (*8*).

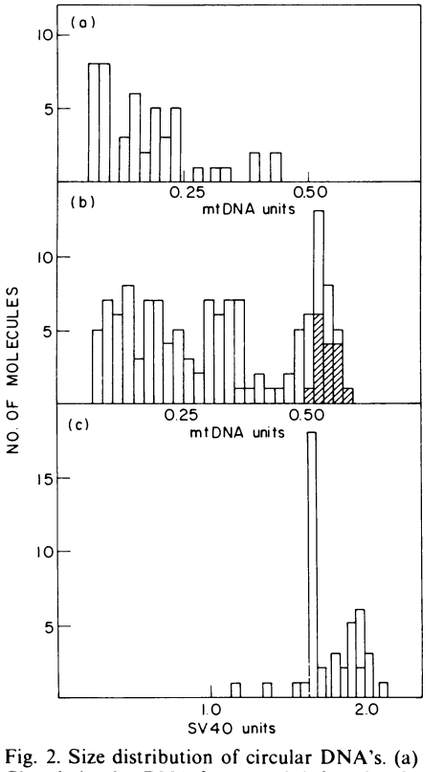

Fig. 2. Size distribution of circular DNA's. (a) Closed-circular DNA from mock-infected JLS-V9 cells was purified by Hirt extraction (*3*) and EtBr centrifugation, and treated with ribonuclease A as in Fig. 1; the surviving closed-circular DNA was isolated by an additional step of EtBr centrifugation. The DNA was nicked with mercaptoethanol (40 m*M*, 12 hours, 37°C) before spreading. All molecules having a length less than that of mtDNA were registered. (b) Infected circular DNA. The DNA was extracted 9 hours after infection and prepared as in (a). The shaded and unshaded bars represent two separate experiments. (c) R_I resistant closed-circular DNA. The DNA was prepared as in (b) and treated with R_I endonuclease (*9*); SV40 DNA was then added as an internal marker. The closed-circular molecules were then isolated by EtBr centrifugation. All molecules other than SV40 unit genomes were scored.

Infected cells show a new size class of circular DNA's. Figure 2b shows the size distribution of circular DNA from two separate preparations. The distribution shown with unshaded bars contains the previously mentioned molecules of 0.1 to 0.4 of an mtDNA unit, as well as a new size class of molecules of 0.52 unit in length. In another preparation (shaded bars), only this new class of 0.52 unit is observed; the smaller sized molecules are absent. Five independent preparations of infected cells have reproducibly demonstrated molecules of 0.52 mtDNA unit. The smaller heterogeneous DNA, as in the mock-infected preparations, is only occasionally present. The molecules of 0.52 mtDNA unit have properties expected of proviral DNA in that they (i) arise as a consequence of infection by M-MuLV, (ii) lack ribonucleotide linkages (*1, 2*), and (iii) are twice the molecular weight of the virion 35*S* RNA subunit and their size is in accord with previous determinations of molecular weight (*1, 2*).

An alternative purification was obtained with R_I endonuclease (*9*). Much of the closed-circular DNA of M-MuLV remains in this form after R_I treatment (*10*). In addition, R_I treatment has only minimal effect on the infectivity of M-MuLV DNA (*11*). These data suggest that the M-MuLV genome might lack cleavage sites for R_I, in contrast to the two known cleavage sites found in mouse mtDNA (*7*).

Treatment with R_I endonuclease followed by EtBr-CsCl centrifugation thus provides a technique useful for the purification of the M-MuLV genome in mouse cells. Electron microscopic survey of the enzyme-treated material showed quantitative removal of closed-circular mtDNA. The SV40 circular DNA was added as a size marker after enzyme cleavage. In addition to the SV40 monomer DNA observed in this preparation (Fig. 3b), two other classes of molecules were observed: SV40 dimers and DNA of 1.67 SV40 lengths, which we assume to be the proviral genome. In the absence of added SV40 marker DNA, this preparation of proviral DNA would have been virtually chemically pure. The calculated molecular weight of the proviral genome is 5.7×10^6 with SV40 as a size reference (*12*), and 5.3×10^6 with mouse mtDNA as a size reference (*7*). By comparison, electron microscopy has shown that the molecular weight of the single-stranded 35*S* RNA subunit of the related RD-114 virus was 2.8×10^6 (*13*).

A further demonstration of the viral origin of these molecules was made possible by a technique developed by White and Hogness, who have shown that RNA can be annealed to a DNA duplex in the presence of high concentrations of formamide (*14*). Control experiments confirmed their data by showing that virtually all SV40 nicked-circular DNA bands more densely in an isopycnic gradient after annealing with an excess of SV40 viral RNA in a high concentration of formamide. We have nicked the putative M-MuLV viral DNA and incubated it under identical conditions

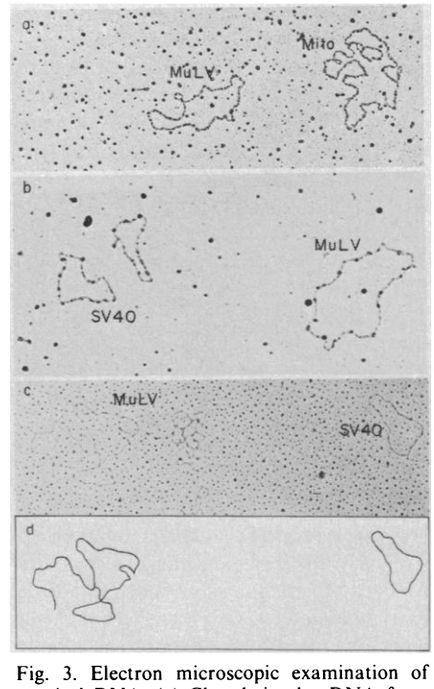

Fig. 3. Electron microscopic examination of proviral DNA. (a) Closed-circular DNA from infected cells was purified as in Fig. 2b, treated with 40 m*M* mercaptoethanol for 12 hours, and examined with variations of the conventional Kleinschmidt technique with a 0.25*M* ammonium acetate hypophase and a 0.5*M* ammonium acetate spreading solution as described (*16, 17*). (b) R_I resistant closed-circular DNA from infected cells was prepared as in Fig. 2c, mixed with a 100-fold excess of form I of SV40 DNA, and visualized as in (a) above. (c) Annealing of viral RNA to circular DNA. The mixture of R_I resistant DNA and SV40 DNA (Figs. 2c and 3b) was treated with mercaptoethanol as above and annealed with 35*S* M-MuLV RNA (40 μg/ml) in 70 percent formamide, 0.5*M* NaCl, 0.1*M* tris (*p*H 7.5) at 50°C for 12 hours (*14*). The mixture was then visualized with a 50 percent formamide spreading solution over a 20 percent formamide hypophase (*16*). (d) A tracing of the MuLV and SV40 molecules of (c).

with a 100-fold excess of M-MuLV 35*S* RNA.

Many of the DNA circles with a molecular weight of 5.5×10^6 now appear to contain single-stranded tails. None of the nicked SV40 molecules, present in the same mixture in 100-fold excess, had any detectable tails. These single-stranded tails have not been well characterized. They may be a mixture of viral RNA and strands of viral DNA partially displaced from the DNA duplex by the annealed viral RNA. They have only been observed after annealing with viral-specific RNA. These tails were derived from the presence of viral RNA and thus constitute additional evidence of the viral origin of the DNA with a molecular weight of 5.3×10^7 to 5.7×10^6.

Electron microscope observation has been necessary to determine the purity of the proviral DNA. The chemically pure proviral DNA should now make possible detailed characterization of its structure.

A. M. GIANNI, J. R. HUTTON*
D. SMOTKIN, R. A. WEINBERG
Center for Cancer Research and
Department of Biology, Massachusetts Institute of Technology, Cambridge 02139, and *Department of Biological Chemistry, Harvard Medical School, Boston, Massachusetts 02115*

References and Notes

1. R. V. Guntaka, B. W. J. Mahy, J. M. Bishop, H. E. Varmus, *Nature (London)* **253**, 507 (1975).
2. A. M. Gianni, D. Smotkin, R. A. Weinberg, *Proc. Natl. Acad. Sci. U.S.A.* **72**, 447 (1975).
3. B. Hirt, *J. Mol. Biol.* **26**, 365 (1967).
4. R. Radloff, W. Bauer, J. Vinograd, *Proc. Natl. Acad. Sci. U.S.A.* **57**, 1514 (1967).
5. M. Miyaki, K. Koide, T. Ono, *Biochem. Biophys. Res. Commun.* **50**, 252 (1973); F. Wong-Staal, J. Mendelsohn, M. Goulian, *ibid.* **53**, 140 (1973); L. I. Grossman, R. Watson, J. Vinograd, *Proc. Natl. Acad. Sci. U.S.A.* **70**, 3339 (1973).
6. J. O. Bishop, J. G. Morton, M. Rosbash, M. Richardson, *Nature (London)* **250**, 199 (1974).
7. W. M. Brown and J. Vinograd, *Proc. Natl. Acad. Sci. U.S.A.* **71**, 4617 (1974).
8. C. A. Smith and J. Vinograd, *J. Mol. Biol.* **69**, 163 (1972).
9. J. Hedgpeth, H. M. Goodman, H. W. Boyer, *Proc. Natl. Acad. Sci. U.S.A.* **69**, 3448 (1972).
10. S. Rozenblatt and R. Weinberg, in preparation.
11. D. Smotkin, A. M. Gianni, S. Rozenblatt, R. Weinberg, *Proc. Natl. Acad. Sci. U.S.A.*, in press.
12. 3.4×10^6 daltons; J. Vinograd, personal communication.
13. H. J. Kung, J. M. Bailey, N. Davidson, M. O. Nicolson, R. M. McAllister, *J. Virol.* **16**, 397 (1975).
14. R. L. White and D. S. Hogness, in preparation.
15. P. A. Sharp, B. Sugden, J. Sambrook, *Biochemistry* **12**, 3055 (1973).
16. C. S. Lee, R. W. Davis, N. Davidson, *J. Mol. Biol.* **48**, 1 (1970).
17. C. S. Lee and C. A. Thomas, Jr., in *Methods in Enzymology*, L. Grossman and K. Moldave, Eds. (Academic Press, New York, 1974), vol. 29E, pp. 443–451.
18. Supported by National Cancer Institute grants CA-14051 and CA-17537, by American Cancer Society grant VC-140, by grants to Dr. C. A. Thomas, Jr., whom we thank for advice and support, by American Cancer Society postdoctoral fellowship PF-958 to J.H., and a research scholar award of the American Cancer Society Massachusetts Division to R.A.W. We thank Dr. White and Dr. Hogness for the communication of their techniques prior to publication.
* Present address: Department of Biology, Marquette University, Milwaukee, Wisconsin 53233

2 September 1975; 14 October 1975

Antileukemic Principles Isolated from Euphorbiaceae Plants

Abstract. *Extracts of* Euphorbia esula *L. and* Croton tiglium *L., two members of the Euphorbiaceae which have been used widely in folk medicine for treating cancers, showed antileukemic activity against the P-388 lymphocytic leukemia in mice. Systematic fractionation of the extract of* Euphorbia esula *L. led to characterization of a major antileukemic component as the new diterpenoid diester, ingenol 3,20-dibenzoate. Similar fractionation of* Croton *oil led to characterization of phorbol 12-tiglate 13-decanoate as an active principle.*

Plants of the family Euphorbiaceae have been used to treat cancers, tumors, and warts from at least the time of Hippocrates (circa 400 B.C.), and references to their use have appeared in the literature of many countries (*1*). We report the isolation and characterization of antileukemic principles from *Euphorbia esula* L. and *Croton tiglium* L., two members of the Euphorbiaceae which are among those used widely in folk medicine (*1*).

In the course of our search for tumor inhibitors from higher plants, we found that an alcohol-water (95 : 5) extract (at room temperature) of *Euphorbia esula* L. from Wisconsin (*2*) showed significant inhibitory activity when tested in rodents against the sarcoma 180, Walker 256 carcinosarcoma, Lewis lung carcinoma, and P-388 lymphocytic leukemia (*3*). The fractionation of an active extract led to the characterization of a major antileukemic component as the new diterpene diester, ingenol dibenzoate (**1**). Ingenol dibenzoate shows significant inhibitory activity, at dosages of 130 to 360 μg per kilogram of body weight, against the P-388 lymphocytic leukemia (*3*).

Successive solvent partition of the alcoholic extract of *E. esula* led to concentration of the antileukemic (P-388) activity in the chloroform layer of a chloroform-water partition. Column chromatography of the residue from the chloroform solution on SilicAR CC-7 and subsequent thin-layer chromatography (TLC) on ChromAR were guided by testing for P-388 inhibitory and piscicidal activity. This procedure led to the isolation of ingenol dibenzoate (**1**, 0.0002 percent of the plant weight), a resinous material (*4*) with specific optical rotation at 28°C for the sodium D line ($[\alpha]_D^{28}$) + 268° (*c*, 0.0026, ethanol). High-resolution mass spectrometry (HRMS) (chemical ionization: methane reagent gas) indicated the empirical formula to be $C_{34}H_{36}O_7$ [calculated ($M^+ + H$), 557.252; found, 557.254].

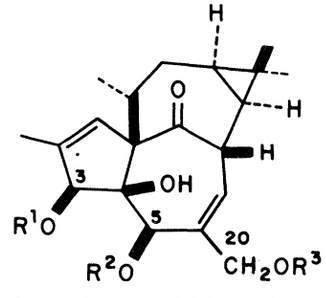

1 $R^1 = R^3 = COC_6H_5$, $R^2 = H$
2 $R^1 = R^2 = R^3 = H$
3 $R^1 = R^2 = R^3 = COCH_3$
4 $R^1 = R^3 = COC_6H_5$, $R^2 = COCH_3$

Spectral data (*5*) suggested that the active principle was a diterpene diester. Accordingly, methanolysis of **1** yielded the tetracyclic diterpene ingenol (**2**), identified by comparison of its spectra with published data (*6*). Acetylation of the methanolysis product afforded the triacetate (**3**; $C_{26}H_{34}O_8$; melting point, 195° to 197°C), which had identical physical constants with those reported (*6*) for ingenol triacetate. The nuclear magnetic resonance (NMR) spectrum of **1** possessed two A_2B_2X systems centered at τ 2.3, indicating the presence of two benzoate groups. This was supported by the mass spectrum of **1**, which contained a strong peak at mass/charge (m/e) 105 (C_6H_5CO).

The structural problem which remained at this point was the determination of the sites of attachment of the two benzoate groups to the ingenol ring system. The NMR signals for H-3 and H_2-20 of **1** appeared at lower magnetic field by 1.46 and 0.82 parts per million, respectively, than the corresponding signals of ingenol (*7*). Acetylation of **1** gave a monoacetate (**4**), and the NMR spectrum of **4** showed the H-5 signal at τ 4.42. These results indicated C-3 and C-20 to be the points of attachment of the two benzoate ester groups. Thus, compound **1** was proved to be ingenol 3,20-dibenzoate.

Our success with *E. esula* prompted us to search for tumor inhibitory principles in an extract of the seeds of a related genus. *Croton* oil, which is the seed oil of *Croton tiglium* L., a leafy shrub native to Southeast Asia, is commercially available (*8*). The diterpenoid esters of *Croton* oil are of current interest as a result of their demonstrated biological activity as cocarcinogens (*9*). When *Croton* oil was evaluated for possible effects on the P-388 lymphocytic leukemia in mice, significant inhibitory activity was noted (*3*). Fractionation of the oil led to the characterization of a major component as the known phorbol diester, phorbol 12-tiglate 13-decanoate (**5**). Com-